Journal of Micromechatronics, Vol. 2, No. 3-4, pp. 185–200 (2004)

Also available online - www.vsppub.com

Micro-scale force-fit insertion

JAMES F. (RED) JONES [1,*], DAVID M. KOZLOWSKI[1]
and JEFFREY C. TRINKLE[2]

[1] *Sandia National Laboratories, Intelligent Systems and Robotics Center, Albuquerque, NM 87185, USA*
[2] *Rensselaer Polytechic Institute, Department of Computer Science, Troy, NY 12180, USA*

Abstract—Several LIGA (Lithography Galvonoforming Abforming) test mechanisms have been designed and fabricated to study tribology and performance attributes of LIGA mechanisms. The LIGA test mechanism studied in this paper is a ratchet drive mechanism consisting primarily of pawls, cams and springs, ranging in size from about one-half millimeter to tens of millimeters, of various nickel alloys fabricated using the LIGA process. To assemble the test mechanism, subassemblies are made by inserting force-fit pins into stacks of piece-parts. These pins are cut from 170 μm wire and range from 500 to 1000 μm in length. Human insertion of these pins is extremely difficult due to their small size and tolerances required to perform the force-fit operation. This paper describes the tooling to permit fabrication, bulk handling and force-fit insertion of pins with the operator-guided automation required to achieve micron-scale tolerances using hybrid force/position control algorithms.

Keywords: Microsystems; LIGA; robotics; force control; fixturing; assembly; force fit.

1. INTRODUCTION

Over the past decade, a great deal of research and development has been devoted to the fabrication of micro-scale devices. Currently, two main technologies are emerging for fabricating micro-scale machines. One technology is polysilicon based and the other is LIGA. The polysilicon devices are fabricated using micromachining techniques leveraged from the integrated circuit industry [1, 2]. The LIGA devices are fabricated using an X-ray lithography technique to make molds into which metallic material may be electroplated [3]. Although polysilicon and LIGA technologies encompass the bulk of the literature, conventional machining techniques are also continuing to evolve to enable millimeter-scale fabrication with micro-scale features [4].

*To whom correspondence should be addressed. E-mail: redjone@sandia.gov

LIGA technology in particular is migrating into many diverse applications and industries. Several applications exist in optical communications including fiber optic alignment, connectors, beam splitters and optical switches [5, 6]. Numerous applications exist in the medical industry including sensors, micro-pumps, micro-turbines, fluidic actuators and separators, nanotiterplates and nanofilters [7, 8]. Potential military applications exist in safety and arming systems [9]. Broad applications exist for a range of gears, sensors, inductors, actuators, transducers, chemical detectors and micro-amplification structures [10–12].

One of the issues with LIGA technology is that the process produces micro-scale parts that need to be assembled into larger subsystems [13]. Consequently, a significant amount of effort has been expended developing the technology to manipulate micro-scale parts individually using micro tweezers or vacuum tools with robotic systems [14–17]. Micro-manipulation is further complicated by the need to integrate sensors into the robotic assembly system in order to achieve the extremely tight positional tolerances required to assemble LIGA structures, mechanisms, or subsystems [18–20]. Some promising work has been performed in the area of parallel assembly both at the wafer level prior to release [21] and using magazines of parts [22] to improve assembly efficiency. Following assembly, many of the resulting structures, mechanisms, or subsystems must be permanently attached to one another using methods such as diffusion bonding [23], selective electroplating [24], anodic, eutectic, or adhesive bonding [25].

One process that is frequently performed in support of micro-system assembly is forcing pins into holes having interference tolerances, which means that the nominal diameter of the hole is smaller than that of the pin. This type of assembly is referred to by several names including force fit, press fit, or interference fit. Standardized tolerances for force fits evolved largely in the first half of the 1900s. The first American Standards Association standard (B 4a-1925) used formulas to determine the tolerances for these fits [26]. In 1926, an international effort began through the International Standards Association to develop international uniformity of tolerances based on practical experience, not on theory [27]. Over the years, a great body of work was published regarding these standards; however, since the standards evolved *via* consensus of experts, no experimental and little theoretical work appears in the literature. Further, publications concerning tolerances for sub-millimeter nominal diameter fits have not been found. The applicable standards such as ISO286 specifically excludes nominal diameters under 1 mm, while ANSI B4.1 does include specifications for sub-millimeter nominal diameters; however, the data in that size scale could be considered questionable because the allowable tolerance can exceed the nominal diameter.

Force-fit insertions may be used to provide shafts for rotating parts or alignment of assemblies. In the case of the LIGA test mechanism, force-fit pins are also used to attach parts together to form subassemblies. These pins are typically significantly smaller than the parts themselves. Consequently, force-fit insertions are extremely difficult because the alignment tolerances are significantly smaller than a human

can achieve using commonly available hand tools and will become more difficult as the sizes of parts continue to decrease. This paper describes the development of a laboratory system that presses pins into force-fit tolerance sub-millimeter size holes.

2. SYSTEM DESCRIPTION

Figure 1 is a photograph of the pin-pressing cell. The pin-pressing cell contains a Physik F-206 hexapod robot with controller, an Eppendorf linear stage, an ATI Nano17 load cell, two Watec CCD cameras, Navitar 5× lenses (with tubes and light sources), video monitor, personal computer, custom fixtures, tooling and software.

The Physik platform was selected for its 6-DOF kinematics with sub-μm resolution and repeatability, thereby making it a good choice for micro assembly research endeavors. Initially, the accuracy of the Physik was characterized in X, Y and Z translations using a laser Doppler displacement meter and then verified with a digital dial indicator. Tests demonstrated that the Physik was accurate to within 5 μm for commanded displacements up to 0.5 mm along these axes. The error increased dramatically as displacement increased. These tests indicated that sensor-based servoing such as vision or force would be required to compensate for displacement errors in order to obtain sufficient positional accuracy.

Although the Physik has sub-micron repeatability and few-micron accuracy, its range of motion is restricted to ± 6 mm in all axes. Consequently, an Eppendorf linear stage was added to the system so that tooling could be moved in and out of the work area. The Eppendorf also possesses sub-micron resolution and repeatability. No study of Eppendorf accuracy was performed because the intended mode of operation only required precise repeatability.

Figure 2 is a schematic that depicts the operation of the cell. LIGA parts are placed in piece part fixtures called disk fixtures to permit easier manual alignment of the

Figure 1. Pin-pressing cell.

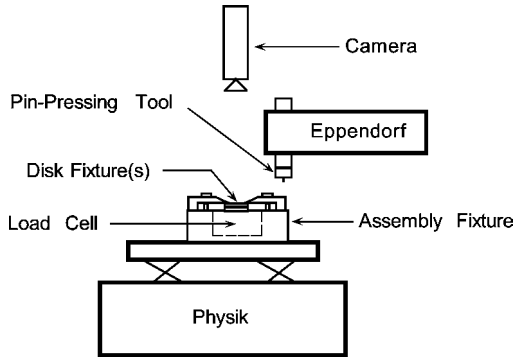

Figure 2. Schematic of pin pressing cell.

parts. The disk fixtures are stacked and clamped in place on the assembly fixture, which is attached to the platform of the Physik robot. The load cell is embedded in the assembly fixture so that pin insertion forces may be monitored. A pin-insertion tool is mounted in a bracket attached to an Eppendorf linear stage. The Eppendorf stage moves the tool into and out of the camera line of sight.

The first operation is to calibrate the pin-insertion tool with respect to the overhead camera. A crude but effective method involved placing a drop of wax on top of the disk fixture. Next, the Physik is maneuvered into position such that the wax is in view of the overhead camera. The Eppendorf is then traversed to a known location so that the pin-insertion tool is positioned within the field of view of the camera. Lastly, the Physik moves the fixtures upward until a pin is inserted into the wax. After insertion, the Physik moves downward and the Eppendorf is retracted. The camera is manually positioned using micrometer stages so that a reticle on the camera monitor is centered on top of the inserted pin.

To insert a pin through a stack of piece-parts, the Physik is moved so that the reticle aligns with the insertion hole. Then the Eppendorf is traversed to its set location and the Physik moves upward until a predetermined force or distance is achieved. Once the pin is inserted, the Physik moves downward and the Eppendorf is retracted. An operator can then assess the success of insertion by switching to a second camera mounted at an angle (not depicted) with respect to the fixture.

3. PIN FABRICATION, HANDLING AND INSERTION

One significant issue was fabrication and handling of the 170 μm $\times$ 500 μm force-fit pins used in the assemblies. The small scale of these pins excludes individual manual manipulation by all but the most skilled technicians. Even skilled technicians find the task of picking and placing these parts difficult and initiating a force-fit insertion extremely frustrating. A better solution would be to maintain pin alignment during pin fabrication through fixturing and tooling followed by staging the pins into magazines.

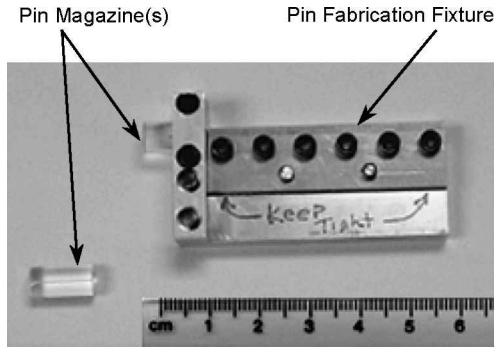

Figure 3. Pin fabrication fixture and magazine.

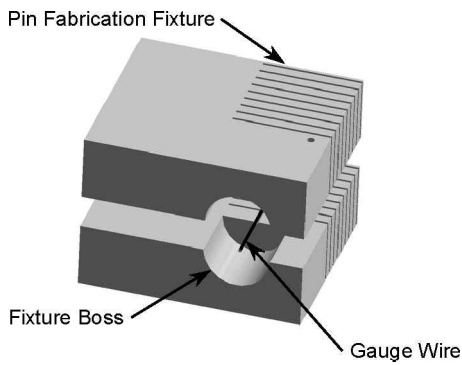

Figure 4. Model of fixture.

Figure 5. Cut pin.

Figure 3 shows a photo of the pin fabrication fixture with pin magazines and Fig. 4 shows a model of the fixture. The fabrication fixture holds a 170 μm diameter gauge wire, while a wire EDM cuts the gauge wire into 500 μm or 1000 μm segments. Once cut, these segments, or pins, are inserted into the glass capillary tube magazine attached to a boss on the fabrication fixture. Figure 5 is a high magnification photo of a cut pin, Fig. 6 shows a scanning electron microscope image of a cut pin and Fig. 7 is a photo of a pin entering the funneled entrance of a magazine.

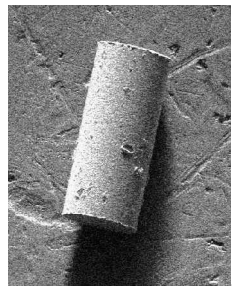

Figure 6. SEM image of pin.

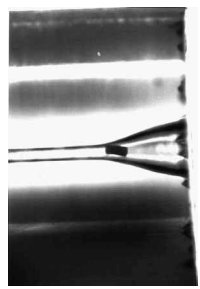

Figure 7. Pin entering magazine.

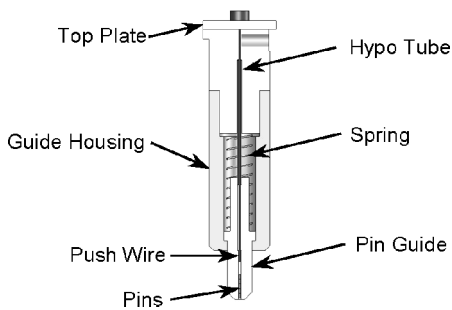

Figure 8. Model of pin-insertion tool.

Figure 9. Photo of pin-insertion tool.

Figure 8 shows a model of the pin insertion tool, while Fig. 9 shows a photograph. The protrusion on the bottom of the tool is a spring-loaded pin guide with an approx. 185 μm through-hole (bore), which is slightly larger in diameter than that of the pins. A push wire, made from the same gauge wire as the pins, butts against the top plate of the tool and runs down into the bore of the spring-loaded pin guide. To prevent buckling, a stainless hypo-tube surrounds the push wire over a majority of its span.

To load the tool, an alignment collar is inserted over the pin guide and the pin magazine is inserted into the other end of the collar. Pins are then inserted into the bore of the pin guide using a long section of gauge wire. Once loaded, the tool is placed in an alignment bracket mounted on the end of the Eppendorf. Pins do not fall out of the tool because the micro-forces (electromagnetic, electrostatic, surface tension, Van der Waals, etc.) dominate gravitational forces at this scale [28]. During pin insertion, the parts to be pinned are moved upward by the Physik into contact with the pin guide. Once contact is made, the pin guide retracts into the guide housing as the parts move upward while the pins remain stationary in the tool, held in place by the push wire backed by the top plate. The difference in diameter between the guide and the housing is about 20 μm. Ultimately, the pin guide continues to retract while the parts move upward until a pin is inserted into the part stack.

The pin insertion tool described above is the second of four prototypes designed, three of which were built. The first prototype worked in a similar manner but held only one pin. The third and fourth prototypes used a side-loading concept that permitted easier loading of larger numbers of pins. The second prototype was considered superior for this application because it could accommodate the wide range of pin lengths necessary for the test mechanism's various subassemblies.

4. FIXTURING

To prepare for pin pressing, a pawl and washer have to be stacked and positioned to align the pair of press-fit holes on both parts. This stacked arrangement has to be maintained while pressing the first pin so that the holes remain aligned for the insertion of the second pin. To simplify manipulation, each part is inserted into a 22-mm diameter stainless steel disc fixture (Fig. 10). The disc fixture is lapped to a thickness of 2.2 mm, which is slightly less than the thickness of a

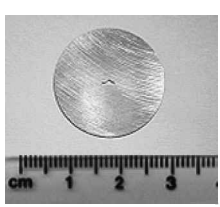

Figure 10. Disc fixture.

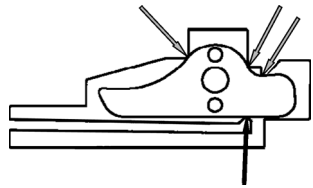

Figure 11. Disc fixture.

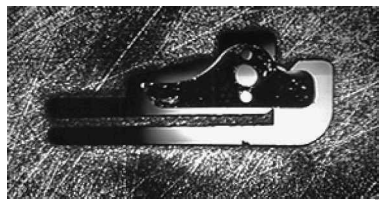

Figure 12. Pawl in fixture.

part. Manual alignment of the fixtures would be an undesirable mass production process; however, the process did prove reasonably easy for a skilled technician using a microscope and completely adequate for the task of assembling prototype mechanisms.

To date, two fixture design philosophies have been applied. The first philosophy was to cut a hole in the center of a disk that matched the shape of the part plus 10 μm of clearance. While intuitive, this approach led to part jamming and cocking during loading or excessive slop during assembly due to lot-to-lot dimensional variations of the parts. In addition, the test mechanism contains three pawl geometries, which would require three different fixtures resulting in escalating fixture costs. These problems were most severe for the pawls, so a new type of fixture was designed for them.

Figure 11 shows the design of the improved pawl fixture disk, while Fig. 12 shows the pawl properly seated inside. The three light arrows point to the fixture contact points. These three contacts were chosen for two reasons. First, they touch a portion of the pawl boundary that is the same for the three pawl designs. Second, they (locally) uniquely position and orient the pawl as long as the contacts are maintained. The fourth contact, indicated by the dark arrow, is at the end of a cantilever beam spring. The location of this contact was chosen so that pushing at that point would seat the pawl against all three fixed contacts.

There are three primary theoretical bases behind the choice of contact locations. The first, restraint analysis, was developed by Reuleaux in 1876 [29], who showed that (locally) unique positioning and orienting of a planar part will be achieved if the part maintains contact with three 'linearly independent' points fixed in space. The second theoretical basis (also due to Reuleaux) for fixture design was used to determine the location of the contact point on the cantilever beam. It was chosen to achieve what Reuleaux called form closure. A part is in form closure if by fixing the contact points the part cannot move (at least four fixels are required for planar

parts) [30]. The third theoretical consideration in the design of the contact point locations is dynamic fixture loading analysis developed recently by Balkcom *et al.* [31]. This analysis assumes that the part is nearly in its properly seated configuration and then determines the set of generalized forces (forces and moments) that are guaranteed to achieve contact with the intended fixels. The design concept was to arrange the three top fixels such that the size of the pushing region was maximized. Then the contact point for the cantilever beam was chosen to lie near the center of the pushing region.

The beam geometry was optimized to generate maximum force for seating the pawl and allowing the maximum spring deflection to ease loading while assuring the beam stress remained below the yield stress of the fixture material. The relation used to perform the optimization was derived from beam stress and defection theory [32–34] for maximum stress,

$$\sigma_{\max} = \frac{3y_{\max}Eh}{2l^2}, \tag{1}$$

where $y_{\max}$ is the maximum deflection, E is the modulus of elasticity, h is the height and l is the length of the beam. Equation (1) was then used to computationally iterate the beam geometry given the constraints that the fixture is stainless steel, a deflection of about 0.15 mm is desired and permanent deformation should not occur. The fixture shown in Fig. 11 has a nominal beam height of 0.22 mm and length of 3.7 mm. When loaded the beam is deflected nominally 0.08 mm, which results in a force applied to the pawl of about 0.17 N. This configuration proved adequate.

5. INSERTION CONTROL

In order to characterize the force fit pin insertion process, many experiments were performed to correlate insertion force with insertion distance.

The first task was to accurately determine the spring constant of the insertion tool's retractable pin guide. Figure 13 shows a plot of manipulator position versus compression force of the pin insertion tool. The data was recorded in 5-μm increments. The spring constant can readily be measured as 1.4 N/mm. In addition, the insertion tool starts to experience a slight degree of non-linear jitter past about 4 mm of compression. This nonlinear behavior is most likely due to the stiction of the pin guide as it slides into the tool housing.

The second task was to insert a pin while continually monitoring the forces in order to determine the required force threshold for reliable pin insertion. Tests demonstrated that to attain full pin insertion a force of as much as 22 N is required. Visual inspection revealed that since the pins are not chamfered (manually chamfering pins of this size is extremely cumbersome), burrs were created during insertion causing the forces to be much larger than originally anticipated and prevented the pin from being inserted completely flush with the surface of the part. Further, the holes in three parts were measured using an optical comparator

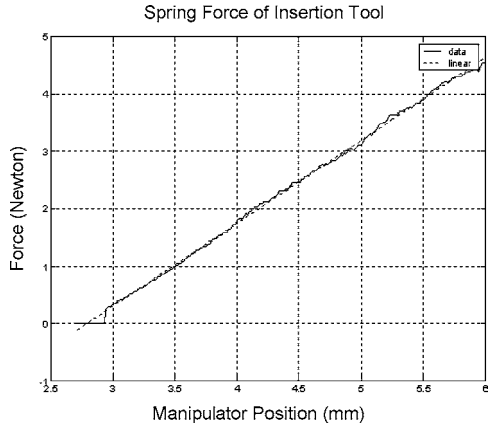

Figure 13. Spring force of insertion tool.

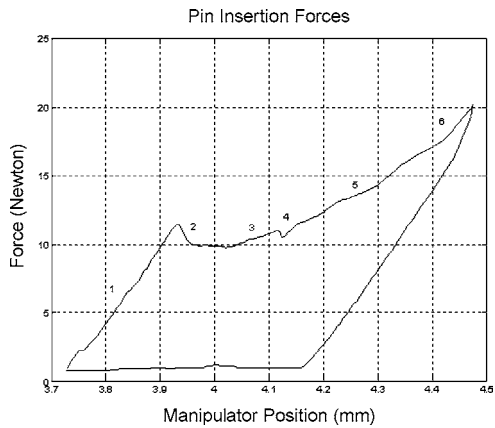

Figure 14. Pin insertion forces.

and found to range from 162 to 165 μm. The pins were fabricated from gauge wire and have a certified diameter of 170 to 171 μm. Thus, the fit has excessive interference, which aggravates the burr formation problem. Experiments with 167.5 μm and 165 μm diameter pins showed that using 167.5 μm diameter pins improved insertion while achieving reliable assembly. In addition, shorter pins were fabricated so that sufficient volume was available at the bottom of the bore for burr compression.

Figure 14 shows a plot of insertion force *versus* manipulator position for the insertion of a pin in a two-part stack-up. One interesting observation is that the manipulator exhibits significant compliance as forces increase as shown in region 1 of the force plot. The actual length of the pin is 500 μm, yet the controller reported a displacement of nearly 750 μm from initial contact to full pin insertion. The plot in Fig. 14 is divided in six sections as described below.

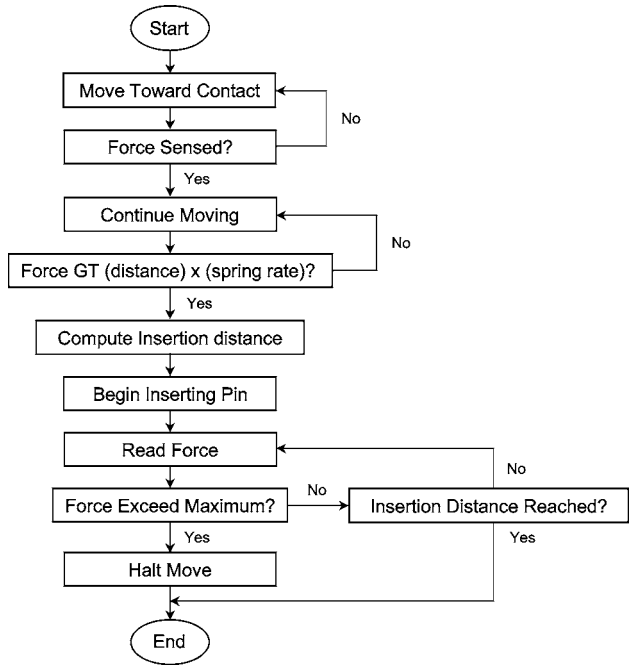

Figure 15. Position/force control algorithm.

1. Forces are increasing gradually as the manipulator is moving upward. The pin has not started to insert into the hole of the first part and compliance is being taken up within the manipulators. Note that the spring rate is about 60 N/mm, which is far in excess of the 1.4 N/mm of the spring loaded pin guide.
2. The pin breaks through into the hole and a burr is created.
3. Point of contact with the second part; forces increase as the pin is forced against the second part before it breaks through.
4. The pin breaks through into the hole of the second part creating a new burr.
5. Forces are increasing while the pin is pressed into the two parts. Material from burr formation is building up at the bottom of the pin and being compressed between the pin and the base fixture.
6. The sudden increase in slope indicates that compression of the burr is complete and no further insertion is possible.

Based on the characteristics of the system a simple position/force control algorithm was implemented (Fig. 15). Once the hole and pin are aligned, the Physik is commanded upward in small increments until force readings indicate that the insertion tool pin guide is compressing and a pin makes contact with the part surface. This location is stored so that the move to contact location for the next pin can be calculated making the guarded move required only once per charge of pins. Once contact is detected, the Physik is commanded to move upward a distance equal to

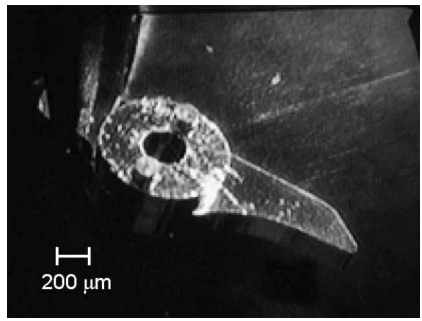

Figure 16. Completed assembly.

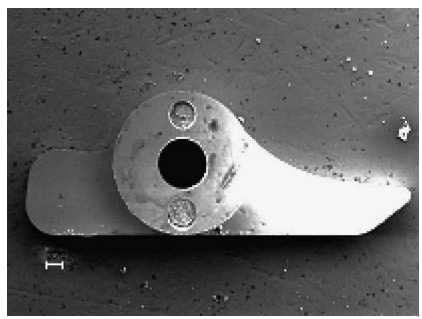

Figure 17. SEM image.

the length of the pin plus a compliance compensation displacement. During the insertion, the controller monitors force and terminates the insertion if a set force is detected prior to reaching the commanded distance.

Figure 16 shows a completed assembly with a washer on top of a pawl. The pins are shown slightly above flush on either side of a center bore. The system was used to insert about 100 pins in support of the test vehicle assembly project. Meaningful data concerning the fraction of successful *versus* failed insertions do not exist because insufficient quantities of pins were inserted within a single controlled experiment to be able to generate statistics with any sort of confidence level. However, qualitatively the initial success rate was under 50% until issues relating to calibration, targeting and manipulator repeatability were addressed. After startup, success improved and declined in direct relation to the success of on-going experiments with pin diameters, fixtures, tooling, etc. Ultimately, a success rate of about 90% was achieved. In the majority of the failures, it was possible to take corrective action, which resulted in the successful fabrication of the assembly.

Figure 17 shows a scanning electron microscope image of an assembly. Careful examination of the lower portion of the bottom insertion hole shows that the edge of the hole was beveled during insertion. The likely cause is that the pin began to be inserted slightly off axis with the hole, as force was applied the pin tended to self-center, due primarily to the clearance in the insertion tool bore and mechanism. This

would indicate that better assemblies and reduced insertion force could be achieved by using pins with chamfered ends and by properly designing compliance into the system [35].

6. CONCLUSIONS

This paper described the tooling, fixturing, control and integration of a laboratory quality micro-scale force-fit insertion robot system. Although the target application for this system is assembly of LIGA components, much of the methodology could be directly applicable to other micro-system assembly issues such as MEMS packaging.

Development and experimentation with the system revealed many ideas that worked and others that need improvement. A pleasant realization was that robotics suitable for many micro assembly operations are commercially available although improved controls systems and larger working volumes could greatly simplify integration. An unexpected discovery was the amount of compliance that exists in the Physik robot at the micro scale, even though the mechanism is based on a Stewart platform, which possesses significant inherent stiffness. Consequently, these proportionally large mechanical deflections necessitated implementing a simple hybrid force/position insertion methodology. In addition, the spring-loaded disk fixture significantly improved the usability of the fixtures and effort required for fixture design and fabrication.

Although the system functions adequately for laboratory applications, a few aspects require resolution before such a system would be suitable for low volume production applications. The most significant issue is that the current calibration procedure requires the skill and patience of a talented technician. Ideally, the calibration methodology would be automated using machine vision. Integrating machine vision into the platform would also enable automated hole location leading to full automation of the process.

The most significant issue needing resolution is that using the square edge pins causes burr formation during the insertion process. The burr results in large insertion forces, entrapped contamination and can cause incomplete insertion. Currently, chemical chamfering of the pins is being investigated. In addition, the possibility of moving from a force fit process to a riveting process is being considered. Even if riveting proves to be a preferred method for attaching piece-parts, force fits will likely remain applicable for bearing shafts and alignment pins in the foreseeable future. Hence, extending the standardized cylindrical fits to sub-millimeter nominal dimensions would be a valuable pursuit.

Acknowledgements

The authors would like to thank Jim Bailar, Dick Shaw, Charleene Lennox, Jim Tauscher, Cliff Loucks, Dannelle Sierra, Diego Lucero and John Feddema for their

assistance in development of this system. Sandia is a multiprogram laboratory operated by Sandia Corporation for the United States Department of Energy under contract DE-AC04-94AL85000.

REFERENCES

1. National Center for Manufacturing Sciences, *Microelectromechanical Systems Manufacturing In Depth*, *Part 1* (2001).
2. National Center for Manufacturing Sciences, *Microelectromechanical Systems Manufacturing In Depth*, *Part 2* (2001).
3. D. Tolfree, Microfabrication using synchrotron radiation, *Rep. Prog. Phys.* **61**, 313–531 (1998).
4. G. Benavides, D. Adams and P. Yang, Meso-scale Machining Capabilites and Issues, *Sandia Report DAND2000-1217C.* Sandia National Laboratories, Alburquerque, NM (2000).
5. W. Ehrfeld and H. Bauer, Application of micro- and nanotechnologies for the fabrication of optical devices, in: *SPIE*, Vol. 3276, pp. 2–14 (1998).
6. A. Muller, J. Gottert and J. Mohr, LIGA microstructures on top of micromachined silicon wafers used to fabricate a micro-optical switch, *J. Micromech. Microeng.* **3**, 158–160 (1993).
7. M. Niggermann, W. Ehrfeld and L. Weber, Fabrication of miniaturized biotechnical devices, *SPIE Conference on Micromach. And Microfab. Process Tech.*, in: *SPIE*, Vol. 3511, pp. 204–213 (1998).
8. W. Menz, Threedimensional microstructures in various materials for medical applications, *IEEE Systems Man and Cybernetics Conference*, Le Touquet, pp. 417–422 (1993).
9. G. Subramanian, M. Deeds, K. Cochran, R. Raghavan and P. Sandborn, Delamination study of chip-to-chip bonding for a LIGA based safety and arming system, *SPIE Conference on MEMS Reliability for Critical and Space Applications*, in: *SPIE*, Vol. 3880, pp. 112–119 (1999).
10. A. Rogner, J. Eicher, D. Munchmeyer, R. Peters and J. Mohr, The LIGA technique — what are the new opportunites, *J. Micromech. Microeng.* **2**, 133–140 (1992).
11. W. Menz, LIGA and related technologies for industrial application, *Sensors Actuators A* **54**, 785–789 (1996).
12. B. Pokines and E. Garcia, A smart material microamplification mechanism fabricated using LIGA, *Smart Mater. Struct.* **7**, 105–112 (1998).
13. J. Hruby, LIGA Technologies and Applications, *MRS Bull.* (April), 1–4 (2001).
14. J. Feddema and R. Simon, *Microassembly of Micro-electro-mechanical Systems (MEMS) using Visual Servoing, Confluence of Vision and Control*, pp. 257–272 (1997).
15. T. Tanikawa and T. Arai, Development of a micro-manipulation system having a two-fingered micro-hand, *IEEE Trans. Robotics Automation* **15**, 152–162 (1999).
16. N. Masayuki, I. Kazahisa, S. Tomomasa and H. Yotaro, Prototypes of micro nontweezing handling tools with releasing mechanisms, *Jpn. Machine Acad. Soc. J. Part C* **61**, 285–290 (1995).
17. W. Zesch, M. Brunner and A. Weber, Vacuum tool for handling microobjects with a nonorobot, in: *Proceedings of the 1997 IEEE International Conference on Robotics and Automation*, pp. 1761–1766 (1997).
18. J. Feddema and R. Simon, CAD-Driven microassembly and visual servoing, in: *Proceedings of the 1998 IEEE International Conference on Robotics and Automation*, pp. 1212–1219 (1998).
19. M. Carrozza, A. Eisinberg, A. Menciassi, D. Campolo, S. Micera and P. Dario, Towards a force-controlled microgripper for assembling biomedical microdevices, *J. Micromech. Microeng.* **10**, 271–276 (2000).

20. Y. Zhou, B. Nelson and B. Vikramaditya, Fusing force and vision feedback for micromanipulation, in: *Proceedings of the 1998 IEEE International Conference on Robotics and Automation*, pp. 1220–1225 (1998).
21. J. Feddema and T. Christenson, Parallel assembly of high aspect ratio microstructures, *SPIE Conference on Microrobotics and Microassembly*, in: *SPIE*, Vol. 3834, pp. 153–164 (1999).
22. M. Nienhaus, W. Ehrfeld, U. Berg, F. Schmitz and H. Soultan, Tools and methods for automated assembly of miniature gear systems, in: *SPIE*, Vol. 4194, pp. 33–43 (2000).
23. T. Christenson and D. Schmale, A Batch Wafer Scale LIGA Assembly and packaging technique via diffusion bonding, in: *12th IEEE International Micro Electro Mechanical Systems Conference*, pp. 476–481 (1999).
24. L. Pan and L. Lin, Batch Transfer of LIGA Microstructures by selective electroplating and bonding, *J. Microelectromech. Syst.* **10**, 25–33 (2001).
25. W. Schomburg, D. Maas, W. Bacher, B. Bustgens and J. Fahrenberg, Assembly for micromechanics and LIGA, *J. Micromech. Microeng.* **5**, 57–63 (1995).
26. A. Vallance and V. Doughtie (Eds), in: *Design of Machine Members*, pp. 456–457. McGraw-Hill, New York, NY (1943).
27. J. Gaillard, ISA Fits, *Am. Mach.*, 616–618 (1936).
28. J. Feddema, R. Simon, M. Polosky and T. Christenson, Ultra-precise assembly of microelectromechanical systems (MEMS) components, *Sandia Report SAND99-0746*. Sandia National Laboratories, Alburquerque, NM (1999).
29. F. Reuleaux, *The Kinematics of Machinery*. Macmillan, London (1876), republished by Dover, New York, NY (1963).
30. J. C. Trinkle, On the stability and instantaneous velocity of grasped frictionless objects, *IEEE Trans. Robotics Automat.* **8**, 560–572 (1992).
31. D. Balkcom, E. J. Gottlieb and J. C. Trinkle, A sensorless insertion strategy for rigid planar parts, *IEEE International Conference on Robotics and Automation*, pp. 882–887 (2002).
32. J. Shigley and L. Mitchell, in: *Mechanical Engineering Design*, p. 51. McGraw-Hill, NY (1983).
33. J. Shigley and L. Mitchell, in: *Mechanical Engineering Design*, p. 804. McGraw-Hill, NY (1983).
34. J. Shigley and L. Mitchell, in: *Mechanical Engineering Design*, p. 813. McGraw-Hill, NY (1983).
35. D. Whitney, Quasi-static assembly of compliantly supported rigid parts, *J. Dyn. Syst. Meas. Contr.* **104**, 65–77 (1982).

ABOUT THE AUTHORS

James F. (Red) Jones is a Principal Member of the Technical Staff at Sandia National Laboratories. He received a BS and MS in Mechanical Engineering from Oklahoma State University in 1984 and 1987, respectively. He is a Registered Professional Engineer. In 1981 he became a partner in a start up business that designed and built laboratory oil field testing equipment. In 1987 he came to Sandia to work in a Nuclear Weapon Component design group and participated in the design and production of surety components for several weapon programs. In 1991 he moved to the Intelligent Systems and Robotic Center. Since coming to the ISRC, he worked in the area of nuclear material automated handling systems, automated process development for the protein industry, design and assembly of micro scale mechanisms. James primary research interests are in the areas of robotics, automated systems, and micro systems.

David M. Kozlowski is a graduate of New Mexico State University (BSEE in 1983) and Purdue University (MSEE in 1985). He has been employed with the Sandia National Laboratory since 1985 where he is currently assigned to the Intelligent Systems and Robotics Center. His current research interests are in nonlinear control, interaction control of robotics, parallel mechanisms, and controlling force interactions at the micro-scale. He is also enrolled at the Graduate School of the Electrical and Computer Engineering Department at the University of New Mexico, currently working towards attaining his Doctorate Degree.

Jeffrey C. Trinkle received his bachelor's degrees in Physics (1979) and Engineering Science and Mechanics (1979) from Ursinus College and Georgia Institute of Technology, respectively. In 1987, he received his PhD from the Department of Systems Engineering at the University of Pennsylvania. Since 1987, he has held faculty positions the Department of Systems and Industrial Engineering at the University of Arizona and the Department of Computer Science at Texas A&M University. From 1998 to 2003 he was a research scientist at Sandia National Laboratories in Albuquerque, New Mexico. He is now Professor and Chair of Computer Science at Rensselear Polytechnic Institute in Troy, New York. Prof. Trinkle's primary research interests are in the areas of robotics, multibody dynamics, and automated manufacturing. For more information visit www.cs.rpi.edu/~trink